Performance and emissions of a high-speed marine dual-fuel engine operating with methanol-water blends as a fuel

Jeroen Dierickx[1*], Quinten Dejaegere[1], Jens Peeters[1], Louis Sileghem[1], Sebastian Verhelst[1,2]

[1] Ghent University, Belgium

[2] Lund University, Sweden

* Corresponding author. *E-mail address:* jeroen.dierickx@ugent.be.

Abstract

Dual-fuel (DF) operation with methanol-diesel allows to reduce CO_2 emissions, increase efficiency and decrease NO_x and soot. This paper describes the experimental results with methanol-water (MeOH-W) blends as a fuel, and has three objectives: (1) whether water acts as a knock suppressant, enabling higher diesel substitution ratios, (2) if water can be a measure to control engine-out NO_x emissions given its cooling effect, and (3) to test the effect on brake thermal efficiency (BTE) of a blend of 90% methanol and 10% water by weight, which is interesting from a methanol fuel production cost perspective. Experiments were conducted on a dual-fuel marine Volvo Penta engine with methanol/water weight by weight shares of 50%/50% (MeOH-50), 64%/36% (MeOH-64), 90% /10% (MeOH-90) and 100%/0% (pure methanol, MeOH-100). A maximal increase in BTE of 3.3% and 4.9% were observed when going from respectively MeOH-100 and diesel-only operation to MeOH-50. The maximum methanol energy fraction (MEF) was obtained with pure methanol, equal to 76%, and decreased with increasing water content. NO_x emissions decreased with pure methanol compared to diesel-only operation, and further decreased with increasing water content. It is concluded that MeOH-90 does not harm the BTE of the tested dual-fuel engine; and that MeOH-50 and MeOH-64 were able to reach IMO Tier III NO_x legislation, but at the same time score worse for greenhouse gas reduction potential as less diesel can be substituted by methanol with these blends.

Keywords: dual-fuel, methanol-water blends, methanol, performance

Abbreviations: MeOH-W, Methanol-water; MeOH-XX, Methanol-water blends with XX 50%, 64%, 90% or 100% denoting the amount of methanol by weight in the blend; ICE, Internal Combustion Engine; GHG, Greenhouse Gas Emissions; DF, Dual-Fuel; EGR, Exhaust Gas Recirculation; DSR, Diesel Substitution Ratio; SI, Spark Ignition; RON, Research Octane Number; DO, Diesel-Only; MEF, Methanol Energy Fraction; BMEP, Brake Mean Effective Pressure; HoV, Heat of Vaporization; BTE, Brake Thermal Efficiency; STP, Standard Temperature and Pressure; SPI, Single Point Injection; MPI, Multiple Point Injection; MMF, Methanol Mass Fraction; RR, Replacement Ratio; LHV, Lower Heating Value; HRR, Heat Release Rate

1. Introduction

Worldwide almost 100 000 vessels are running on fossil fuels (mainly diesel and heavy fuel oil) with internal combustion engines (ICEs) [1], responsible for 2.89% of anthropogenic greenhouse gas emissions [2]. As the maritime sector is expected to grow between 25% and 180% by 2050 [3] and as IMO's initial greenhouse gas (GHG) strategy is a 50% reduction in total annual GHG by 2050 [2], the sector is urging for technological innovation. A promising solution for meeting GHG emission reduction targets is changing to renewable fuels while keeping the proven and reliable ICE [4]. Methanol is seen as a viable renewable fuel for ICEs, certainly for applications where high system energy densities are required [5] [6] [7]. This is thanks to several characteristics of methanol: its liquid state at ambient temperature and pressure (making it practical to handle and transport), it is convenient to produce (it is a simple molecule which can be made renewably from biomass feedstocks and renewable electricity) [8] [9], and its excellent engine performance (high efficiency and ultralow emissions) [4] [10] [11].

Over the past decade, several research efforts have been done on dual-fuel (DF) engines with methanol-diesel [12] [13]. Dual-fuel engines allow a gradual fuel transition to renewable methanol: when methanol is not available for bunkering in a port, vessels can still run on diesel [14]. Different demonstration projects have furthermore proven the technology readiness of dual-fuel engines with methanol-diesel: with low speed engines MAN has already powered more than nine vessels [15], with medium speed engines Wärtsilä has several years of operating experience on four engines in the Stena Germanica [16], and on a high speed Volvo Penta engine dual-fuel operation was demonstrated during the LeanShips project [17]. In the Horizon 2020 FASTWATER project that is currently ongoing, the engine manufacturer Anglo Belgian Corporation nv. will power a tugboat of the Port of Antwerp with two medium speed dual-fuel engines on methanol-diesel [18] [19].

Different concepts exist for dual-fuel engines and they mainly depend on the methanol fuel injection. Methanol can be injected directly in the cylinder into a burning diesel jet [15] [16] or it can be fumigated in the intake manifold, at a single point in the intake or at multiple points before the intake valves [12] [17] [20]. In this paper, the fumigation concept is used as it is the most convenient engine retrofit solution: it has the advantage of a methanol circuit at low pressure and that no engine modifications are required because methanol can be injected in the more easily accessible intake manifold [21].

Although the fumigation concept has been demonstrated and researched over the past decade, challenges remain. Current diesel substitution is mainly limited by knock at high load and misfire at low load [22], but little research has been done on extending these limits. Yao et al. has tested the knock limiting properties of Exhaust Gas Recirculation (EGR) and achieved a 2% increase in diesel substitution ratio (DSR) [23]. Dierickx et al. [21] compared two methanol injection strategies: at high load lower DSRs were reached with a single point methanol injection than with a multiple point methanol injection. Water is known to be a knock suppressant from experiments on spark ignition (SI) engines [4] [24] [25]. Most and Longwell investigated on a single cylinder CFR engine the research octane number (RON) of pure methanol and blends with 5% and 10% water by volume. They found that water increased the RON from 109.6 (pure methanol) to 114 (methanol with 10% water by volume). A first objective of this paper is therefore to investigate the knock limiting properties of adding water to methanol in order to obtain higher DSRs.

Meeting current and future emission legislation like IMO Tier III for NO_x is another challenge for the marine sector [26]. Water injection offers the possibility to reduce peak combustion temperatures thanks to its high heat capacity and high heat of vaporization, in this way reducing NO_x formation during combustion

[24] [27]. Sun et al. investigated the effect of direct water injection on the combustion and emissions of a marine diesel engine and achieved up to 55.6% NO_x reductions [28]. On methanol-water (MeOH-W) blends, very little research has been done. Sileghem et al. has tested methanol-water blends up to 10% water by volume and achieved substantial NO_x reductions up to 42% [29]. MAN has tested methanol-water blends to control NO_x on a two-stroke dual-fuel engine: depending on the engine load, 20% to 40% water by volume was required in the methanol-water blend to obtain IMO Tier III [30]. Cho et al. investigated five different methanol-water blends on a light-duty 4 cylinder 2.9l diesel engine: water/methanol volume ratios of 100%/0% (pure methanol), 90%/10%, 60%/40%, 30%/70% and 0%/100% (pure water) [31]. With the 60%-40% blend maximal NO_x reductions of 28% and 11% were achieved compared to respectively the diesel-only (DO) and the pure methanol case. The tested methanol energy fractions (MEFs) were however limited to 40%. The second objective of this paper is hence to investigate the NO_x reduction potential at high MEFs and this on a heavy duty marine dual-fuel engine.

The third objective of this paper is to test the effect on engine performance of "crude methanol", as this would be interesting from a fuel cost production and from an engine efficiency point of view [4]. In the last step of the production process, methanol is distilled from crude methanol with a purity of 90% to a methanol purity of 99.85% on a weight basis according to the standards of the International Methanol Consumers and Producers Association (IMCPA) [32]. Up to 15% of the production cost could be saved by skipping this distillation step compared to the production cost of IMCPA quality methanol [33]. On the engine side, methanol-water blends have the potential to increase engine efficiency thanks to the cooling effect of water [4]. With ethanol in SI engines, several publications have shown that ethanol-water blends (up to 7% weight water content) perform as an efficient fuel [34] [35]. Sileghem et al. found on a 4 cylinder light duty SI engine an increases in efficiency between 1% and 2% for pure methanol and methanol-water blends up to 10% water by volume compared to pure gasoline operation, and no significant difference in efficiency between the different methanol-water blends [29].

In this paper, the above objectives are tested by means of four different methanol-water blends at three different load points. The tested blends had a methanol/water weight by weight share of 50%/50% (MeOH-50), 64%/36% (MeOH-64), 90%/10% (MeOH-90) and 100%/0% (MeOH-100 or thus pure methanol), and they were tested at a speed of 1500 rpm for the brake mean effective pressures (BMEPs) of 3.5 bar, 10.6 bar and 12.3 bar. At each engine load, the amount of methanol-water blend was increased starting from diesel-only operation until the maximum diesel substitution by MeOH-W was reached. In Section 2, the fundamentals of adding water on the dual-fuel combustion process are first described, while in Section 3 the experimental setup and the test procedure are presented. In Section 4, the effect of different methanol-water blends on the maximum MEF and DSR, combustion pressure and heat release, brake thermal efficiency and NO_x are discussed for the tested experiments.

2. Fundamentals of adding water on engine performance

In the dual-fuel engine of this research, two fuels burn: the methanol-air mixture is ignited by the pilot injection and auto-ignition of diesel, after which a complex combustion of these two fuels follows. When mixing water with methanol in order to obtain a methanol-water blend, a third substance is introduced to the cylinder which will affect the combustion process. Before describing the test engine and analyzing the test campaign results, it is therefore important to more fundamentally understand how water changes the compression and combustion behavior in a cylinder. This will help in the analysis in Section 4 to better distinguish the effect of each substance present in the cylinder.

As introduced in Section 1, water is known to suppress knock and to reduce NO_x emissions. This is thanks to its high heat of vaporization and its high heat capacity. When water is evaporated in the intake manifold it evaporates using heat of the intake air and its surroundings (depending on injection position: intake pipe, intake valves, cylinder head, cylinder walls). The intake charge composition changes: water replaces some of the air, but this might be counteracted by the lower intake temperatures leading to higher air density and thus a better filling of the cylinder. Lower intake temperatures mean lower in-cylinder temperatures, mitigating knock and thermal NO_x formation. The high heat capacity of water further decreases in-cylinder temperatures as water vapor has a lower temperature increase than air for the same heat absorption.

The heat of vaporization (HoV) of water and methanol are given in Table 1. In dual-fuel operation the effects of the cooling effect of methanol are known [12] [13] [17]. With regard to the maximum DSR, at high load lower intake temperatures decrease the possibility for pre-ignition and knock [21], but at low load the lower intake temperatures are responsible for misfire at high diesel replacement. The lower in-cylinder temperatures with increasing methanol energy lead to (1) higher brake thermal efficiency (BTE) (especially at higher loads) due to lower heat losses and a more rapid combustion, and to (2) lower NO_x formation. As the HoV of water is higher than for methanol, it can thus be expected that the cooling effect of MeOH-W blends are higher than for pure methanol. It is expected that this further decreases NO_x, increases BTE, and extends the diesel substitution limits at high load. In Table 1, the specific heat capacity (c_p) of water and methanol (in their liquid and gaseous phase) and air are shown. The heat capacity of the intake charge is an important characteristic during the compression stroke. Water vapor has a higher heat capacity than air and gaseous methanol. With increasing water content in the MeOH-W blend and for equal methanol energy content, it can thus be expected that the heat capacity of the intake charge will increase and further decrease in-cylinder temperatures.

Substance	**Heat of vaporization, HoV** [kJ/kg]	**Heat capacity, c_p (at STP)** [kJ/kgK]
Water, liquid	2454	4,184
Water, vapor	n.a.	1,996
Methanol, liquid	1165	2,54
Methanol, gaseous	n.a.	1,632
Air	n.a.	1,006

Table 1: Heat of vaporization and heat capacity of methanol, air and water.

3. Dual-fuel test setup

During the Horizon 2020 project LeanShips, a high speed marine diesel engine, a Volvo Penta D7C-B TA, was converted to dual-fuel operation to demonstrate the potential of methanol as a marine fuel. The results of the first measurement campaign have been published in [17]. In [21], two different methanol injection strategies were compared: a single point injection (SPI) of methanol in the intake duct and a multiple point injection (MPI) just before each valve of the six cylinders. In this paper, the MPI strategy has been used for injecting MeOH-W blends. A schematic overview of the setup can be seen in Figure 1.

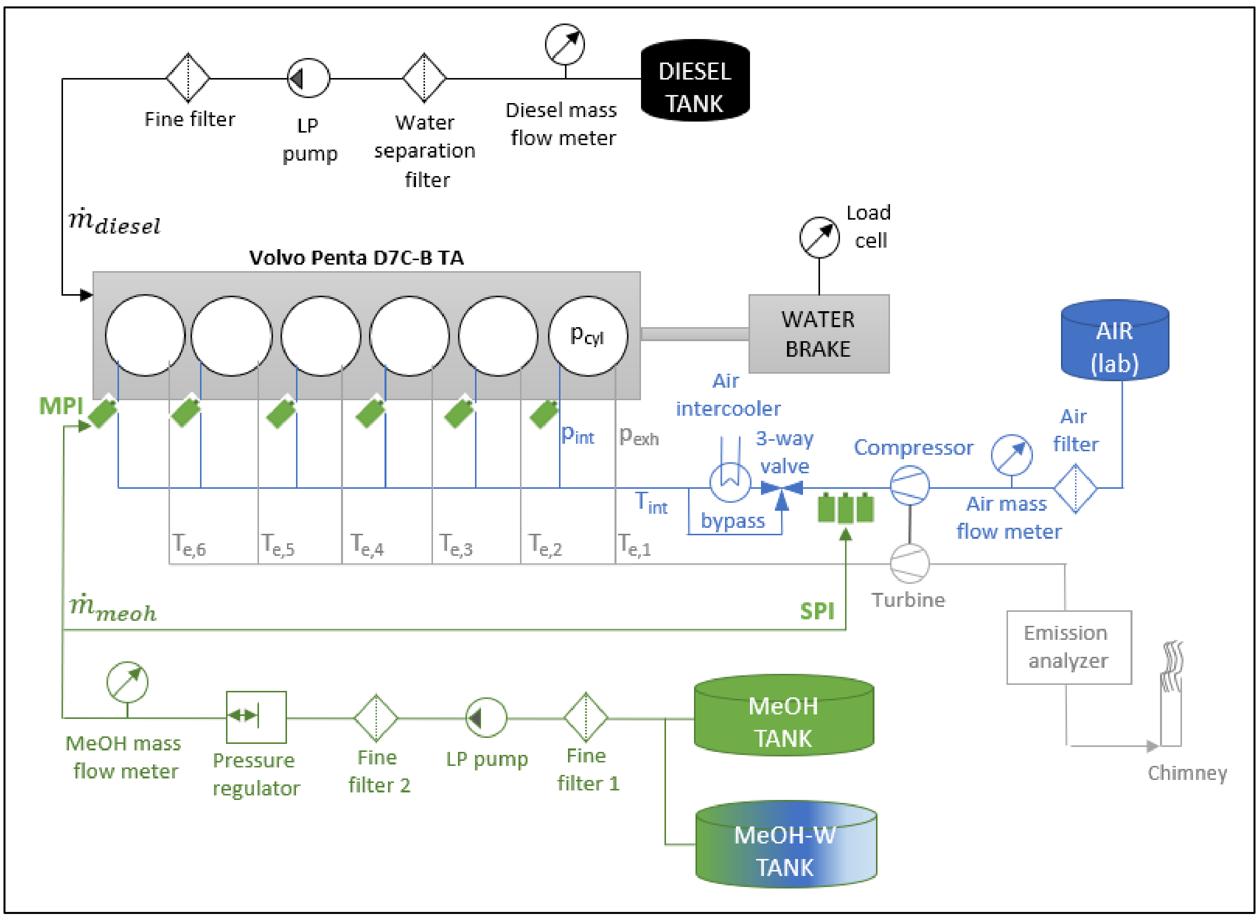

Figure 1: Schematic view of the Volvo Penta D7C-B TA converted to dual-fuel operation.

Table 2 summarizes the technical specifications of the Volvo Penta engine converted to dual-fuel operation and Table 3 the details of the methanol supply system and the measurement equipment. For a detailed elaboration of the engine conversion and its design, the reader is referred to [21]. For the MeOH-W blend tests that were conducted in this paper, an additional tank was added to the setup as can be seen on Figure 1. When dual-fuel operation was changed from pure methanol to MeOH-W blends, the fuel intake line was decoupled and coupled to the MeOH-W tank.

Volvo Penta	
Model	D7C-B TA
Aspiration	Turbocharged with air intercooler
Cylinders	6, in-line
Compression ratio	19.0
Bore x stroke	108 mm x 130 mm
Displacement volume	7,15 l
Diesel injection system	Cam-driven Single Injection Pumps
Diesel injection pressure	1200 bar
Maximum torque / speed / bmep	904 Nm / 1500 rpm / 15.9 bar
Rated power / speed / bmep	195 kW / 2300 rpm / 14.2 bar

Table 2: Technical specifications of the Volvo Penta, D7C-B TA, converted to dual-fuel operation.

Methanol supply system	
Injectors	Bosch EV14 CKxT
Pump & filters	Fuelab pump (41401c) & filters (60 & 75 µ)
ECU	Motec M800
Measurement equipment	

Mass flow	Bronkhorst M15 (diesel & meoh) & F (air)
Pressure	Keller M5HB (low p) & Kistler 6045B (high p)
Temperature	K-type (high T) & J-type (low T)
Load	Logicontrol H3
Data acquisition	NI DAQ 9205, 9213, 9215, 9401, Labview
Emissions	MAIHAK Unor 610

Table 3: Methanol supply system and measurement equipment details.

The MeOH-W blends were made on a weight by weight basis using a METTLER Toledo ICS429 weighing platform (with an accuracy of 0.001 kg). To make the blend, the following steps were performed: (1) verifying the purity of methanol with a pycnometer, (2) calibration of the weighing platform, (3) weighing the barrel and the rack, (4) addition of methanol to the barrel, (5) addition of water to the barrel. Steps (4) and (5) were continued until the desired methanol-water ratio was reached (see Section 4).

4. Methodology

4.1 Definitions

In dual-fuel operation, it is important to accurately describe the amount of each fuel that is used at any moment. Different definitions are used – the main four being the methanol energy fraction (MEF), the diesel substitution ratio (DSR), the methanol mass fraction (MMF) and the replacement ratio (RR) [21]. In this paper, MEF is mainly used as it indicates the amount of energy coming from methanol in comparison to the total amount of energy in the cylinder. DSR is applied when the amount of diesel replaced by methanol is important, as this is a measure for the CO_2 reduction potential when renewable methanol is used. Both definitions are shown below, with DO and DF standing for respectively diesel-only and dual-fuel, and $\dot{m}$ and LHV being respectively the mass flow and the lower heating value of the respective subscripts.

$$MEF = \frac{\dot{m}_{MeOH} \cdot LHV_{MeOH}}{\dot{m}_{MeOH} \cdot LHV_{MeOH} + \dot{m}_{Diesel} \cdot LHV_{Diesel}}$$

$$DSR = \frac{\dot{m}_{diesel\ in\ DO} - \dot{m}_{diesel\ in\ DF}}{\dot{m}_{diesel\ in\ DO}}$$

The amount of diesel that can be substituted by methanol is typically limited by one of the following four boundaries [22] [21]: at low load by misfire or partial burn; and at high load by roar combustion, knock, exceedingly high exhaust temperatures or methanol pre-ignition. In Section 5.2 the maximum MEF and DSR will be discussed as a function of the amount of MeOH-W.

In this paper the different MeOH-W blends are abbreviated by MeOH and a number. For example MeOH-50 points to a blend with 50% methanol and 50% water by weight. As the MeOH-W blends in this research are always on a weight by weight basis, this will not be explicitly mentioned each time.

In Section 5, different parameters are discussed such as in-cylinder pressure and temperature, heat release rate (HRR), and combustion phasing (CA10, CA50 and combustion duration). For the in-cylinder pressure the best fitted pressure trace from 100 measured cycles was used for the analysis in Section 5. To select the best fitted pressure trace first the average pressure cycle was calculated. The pressure trace that was closed to this average cycle was then selected. The HRR was calculated following the first law of thermodynamics:

$$\frac{dQ}{d\theta} = \frac{\gamma}{\gamma - 1} \cdot P \cdot \frac{dV}{d\theta} + \frac{1}{\gamma - 1} \cdot V \cdot \frac{dP}{d\theta}$$

In this equation Q is the heat release, P the in-cylinder pressure, V the instantaneous volume and θ the crank angle. Gamma was calculated on a crank angle basis, based on the mixture's gas properties during the cycle: the heat capacity and the specific gas constant were calculated for the burned and unburned mixture, and during combustion a linear regression was applied between both. Based on the HRR, the combustion phasing parameters CA10, CA50 and combustion duration (= CA90-CA10) were calculated. The in-cylinder temperatures were calculated based on the ideal gas law and the in-cylinder pressure trace. The diesel injection timing of the Volvo Penta engine was not known, but as the diesel injection system is a pump-line-nozzle system it can be assumed that the injection timing is equal at equal speed. The specific NO_x emissions were calculated according to the IMO Marpol/CONF.3/34 [36].

Taylor's error equation [37] was applied for calculating the measurement uncertainty on the brake thermal efficiency and the NO_x emissions that are presented in respectively Section 5.4 and 5.5:

$$\delta q(x_1, x_2, \ldots, x_n) = \sqrt{\left(\frac{\partial q}{\partial x_1} \cdot \delta x_1\right)^2 + \left(\frac{\partial q}{\partial x_2} \cdot \delta x_2\right)^2 + \cdots + \left(\frac{\partial q}{\partial x_n} \cdot \delta x_n\right)^2}$$

$$BTE = \frac{P_e}{\dot{m}_m \cdot LHV_m + \dot{m}_d \cdot LHV_d}$$

$$\delta BTE^2 = \left(\frac{1}{\dot{m}_m \cdot LHV_m + \dot{m}_d \cdot LHV_d}\right)^2 \cdot \left(\delta P_e^2 + \left(\frac{P_e \cdot LHV_m}{\dot{m}_m \cdot LHV_m + \dot{m}_d \cdot LHV_d}\right)^2 \cdot \left(\delta \dot{m}_a^2 + \delta \dot{m}_d^2\right)\right)$$

$$NO_{(2)(x)} = \frac{NO'_{(2)(x)}}{P_e}$$

$$\delta NO_{(2)(x)}{}^2 = \left(\frac{1}{P_e} \cdot \delta NO'_{(2)(x)}\right)^2 + \left(\frac{1}{P_e} \cdot \delta P_e\right)^2$$

In these equations the subscripts a, m, and d denote air, methanol and diesel respectively; P_e is the brake thermal power and equal to $2 \cdot \pi \cdot Brake\ Torque\ \cdot Engine\ speed$; and $NO_{(2)(x)}$ and $NO'_{(2)(x)}$ the emissions in respectively g/kWh and g/h. The uncertainties on the individual measurements were equal to:

$$\delta \dot{m}_m = \delta \dot{m}_d = 0.2\% \cdot reading\ kg/h$$

$$\delta \dot{m}_a = 0.5\% \cdot reading + 1.225\ kg/h$$

$$\delta(Brake\ Torque) = 0.2\%\ \cdot reading + \ 9.4\ Nm$$

$$\delta(Engine\ Speed) = 5\ rpm$$

$$\delta NO_{(2)(x)} = 1\% \cdot reading + 15\ ppm$$

4.2 Measurement matrix and test procedure

In this paper, pure methanol (as a reference) and three different methanol-water blends were tested in dual-fuel operation. The methanol-water blends weight by weight and there abbreviation are 50%/50% or MeOH-50, 64%/36% or MeOH-64, 90%/10% or MeOH-90, and pure methanol or MeOH-100. MeOH-50 was chosen as at high MEF the specific water content (g_{water}/kWh) is similar to specific water contents used in research with water injection in CI engines. This blend corresponds furthermore close to the reported crude methanol (being 49%/49% water/methanol volume by volume) as an intermediate product from the renewable production process based on water electrolysis and CO_2 hydrogenation [38]. MeOH-64 was selected because it is the composition of crude methanol made renewably from hydrogen and captured CO_2 [39]. The chemical reaction $CO_2 + 3H_2 \rightarrow CH_3OH + H_2O$ denotes that for every mole of methanol, one mole of water is produced which is approximately equal to 64%/36% methanol/water weight by weight. Another reason for selecting MeOH-64 was MAN's research, as mentioned in Section 1, stating that with 20% to 40% water by volume (which is equal to 24% to 45% water by weight) IMO Tier III limits were reached without aftertreatment. The last blend, MeOH-90, was selected to represent the crude methanol composition from the methanol production process out of natural gas or biomass. The composition of crude methanol varies according to the production process, but typically with a water by volume content in the range of 5% to 20% (= 7% to 24% water by weight) [40]. As methanol with a water content up to 10% by weight is reported as not deteriorating engine performance [32], such a blend was thus chosen for this research.

The different MeOH-W blends, MeOH-100-90-64-50, were tested at 1500 rpm and at three BMEPs, namely 3.5 bar (22% full load (FL)), 10.6 bar (66% FL) and 12.3 bar (78% FL). At each load, it was started from diesel-only operation and consequently the amount of MeOH-W blend was increased in small steps (typically ~5%). With increasing MeOH-W injection the diesel mass was decreased to remain at the same load and speed. The amount of diesel was substituted by MeOH-W until one of the limits as described in Section 4.1 was reached.

5. Research results

This paper has (as mentioned in Section 1) three objectives: (1) to look into the knock limiting properties of MeOH-W blends in order to obtain higher DSRs, (2) to investigate the NO_x reduction potential at high MEFs, and (3) to test the effect on engine performance of crude methanol. In the following, we first analyze the in-cylinder temperatures and the maximum obtained MEFs, then the combustion characteristics, and then the efficiency and NO_x emissions.

5.1 In-cylinder temperature

Following the flow from inlet to outlet, the first change when going from diesel-only operation to dual-fuel operation is that methanol is added just before the intake valves: methanol is fumigated in the inlet just before the intake valves. When going from methanol operation to MEOH-W operation, the fumigated characteristics change: with increasing water content and for an equal methanol energy quantity, a higher volume is injected and thus the injection time increases for fixed injection pressure.

The first encountered impact on the engine's operation is that the intake/cylinder temperature and pressure, and air mass flow change due to the displacement effect of the injected MeOH-W and its evaporation. MeOH-W displaces part of the volume that is in DO operation taken by air. Evaporation of MeOH-W cools down the air charge on the other hand and increases the air density enabling a higher air mass flow.

In Table 1, the heat of vaporization (HoV) is given for water and methanol. For MeOH-W blends, the following equation has to be used to calculate its HoV:

$$HoV_{MeOH-W} = HoV_{H2O} \cdot \dot{m}_{H2O} + HoV_{MeOH} \cdot \dot{m}_{MeOH} \quad \left[\frac{MJ}{h}\right]$$

When applying the measurement data at 10.6 bar BMEP with the above equation, Figure 2 is obtained. It can be seen that for example for MEF = 20%, the HoV_{HMeOH} triples from about 10 MJ/h to 30 MJ/h when going from pure methanol to MeOH-50. It can thus be seen that with increasing water content, the cooling effect increases significantly.

Another effect that cools down the cylinder is the heat capacity of the mixture of air and MeOH-W ($c_{p,mix}$). The specific heat capacities of gaseous water and gaseous methanol are respectively 1,996 kJ/kgK and 1,6320 kJ/kgK at ambient temperature and pressure. The heat capacity of water is thus almost double that of air (1,006 kJ/kgK), and that of methanol is about 60% higher than air. During compression, pressure and temperature increase in the cylinder and therefore $c_{p,mix}$ changes as a function of piston position. At TDC and at 10.6 bar BMEP the heat capacity is given in Figure 2. It can be seen that $c_{p,mix}$ increases with increasing MEF from about 1,15 kJ/kgK in DO to about 1,45 kJ/kgK in DF. It can also be seen that for equal MEF, $c_{p,mix}$ increases with increasing water content.

On Figure 2 gamma (γ) at TDC is plotted as well at 10.6 bar BMEP. With higher water content, gamma slightly decreases until a MEF of about 40% beyond which gamma is no longer affected by the water content. From the ideal gas law it can be derived that for an ideal gas the temperature at the end of compression (T_{TDC}) has the following relation to the temperature at the start of compression (T_1):

$$T_{TDC} = T_1 \cdot CR^{\gamma-1}$$

With CR being the compression ratio. From this equation it can be deducted that the higher gamma, the higher the temperature at TDC for an equal T_1. With dual-fuel operation a methanol-air mixture is compressed so this equation cannot be applied. However, it can be assumed that gamma is an indicator for the temperature at the end of compression: a higher gamma leads for equal temperature at start of compression to a higher temperature at TDC, and vice versa.

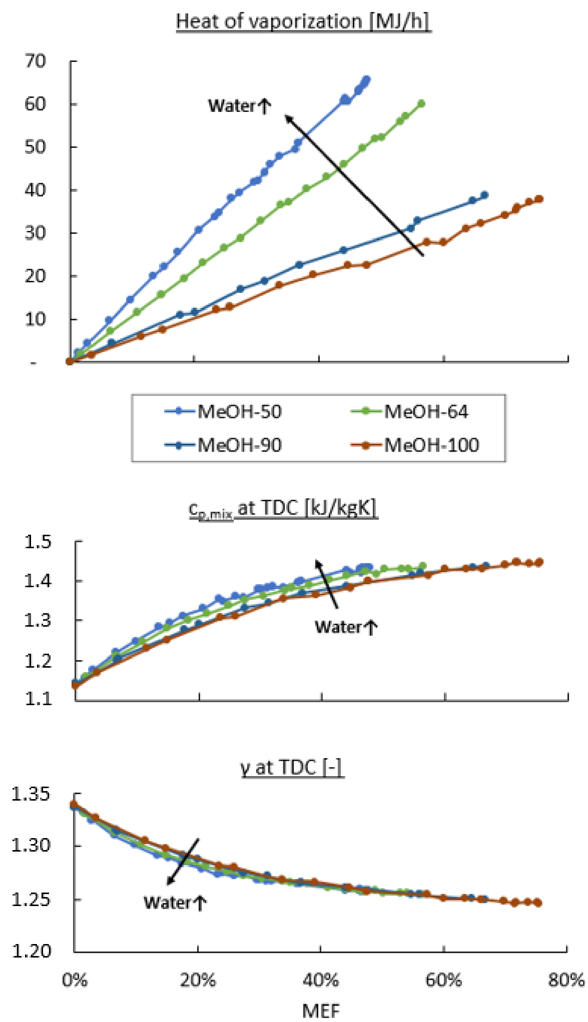

Figure 2: Heat of vaporization, heat capacity and gamma at 10.5 bar BMEP and for different MeOH-W blends and MEFs.

The in-cylinder temperature is calculated based on the measured in-cylinder pressure, assuming thus that the mixture of air and MeOH-W behave as an ideal gas:

$$T_{mix} = \frac{p_{mix} \cdot V}{m_{mix} \cdot R_{mix}}$$

The mass of the mixture equals the sum of the masses of air and MeOH-W. The diesel mass is neglected here as the main purpose is to visualize the temperature into which diesel is injected. Intake charge losses due to scavenging are neglected as well. The specific gas constant of the mixture, R_{mix}, is calculated as a function of the mixture composition. The resulting in-cylinder temperature at TDC is shown in Figure 3. It can be seen that there is a significant decrease in temperature as a function of MEF, and the higher the water content, the lower the temperature at TDC. At 3.5 bar BMEP, all temperatures at TDC vary between 631 and 732 °C and at 12.3 bar BMEP between 633 and 811 °C. The absolute temperature decrease is thus higher with increasing load. With reduced temperatures at TDC (or thus with increasing MEF), it can be expected that the ignition delay will increase, and even more with higher water contents.

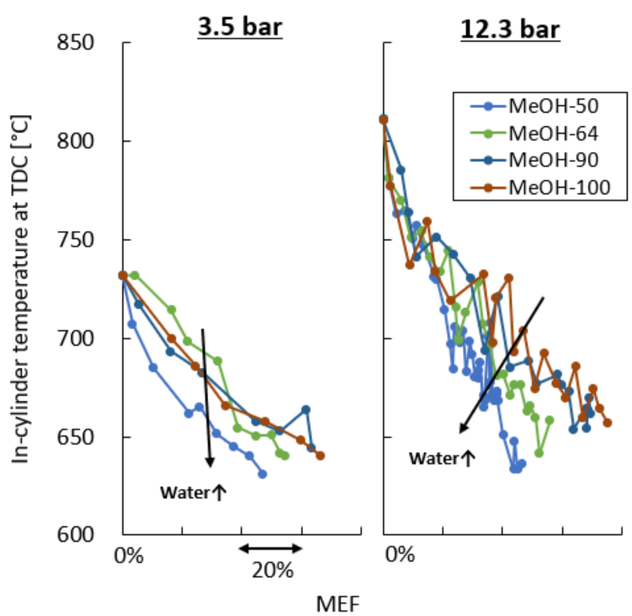

Figure 3: In-cylinder temperature at TDC at 3.5 bar and 12.3 bar BMEP.

5.2 Maximum methanol energy fraction

From earlier research on this engine [17] [21], it is known that at low loads the diesel substitution limit is typically limited by misfire. Misfire is characterized by an excessively long ignition delay due to the increased cooling at high MEF, not making it possible anymore for the diesel to auto-ignite. At high loads the typical diesel substitution limit is diesel or methanol knock. Diesel knock can be characterized by very high pressure rise rates (typically higher than 15 bar/°CA) due to a large amount of diesel that burns premixed. Such a large amount of premixed diesel can originate from long ignition delays. Methanol knock on the other hand is the auto ignition of the unburnt methanol end gases before the methanol flame front (ignited by the diesel pilot) could reach these end gases. For this event to happen, high temperatures and pressures are necessary. One of the causes for such circumstances is a higher share of fuel that burns in the premixed combustion phase, which is possible with longer ignition delays due to the cooling effect of MeOH-W blends. During the measurements knock was detected by ear and during post processing of the data the in-cylinder pressure traces were analyzed. It was seen (see Figure 5) that no pressure oscillations were observed in cylinder 1 (which holds the pressure sensor), nor pressure rise rates higher than 15 bar/°CA (maximum 10.8 bar/°CA), meaning that the knocking event occurred in one of the other six cylinders. As these cylinders did not have a pressure measurement, it was not possible to pinpoint the cylinder with knock and to distinguish diesel from methanol knock. Thus, when knock is mentioned below it can be either type of knock.

On Figure 4 the maximum MEF is shown as a function of load and water content. The error on the MEF is of the order of 0.1% and therefore not shown. It can be seen that the highest MEF is reached at 10.6 bar BMEP with pure methanol, while the lowest MEF is reached at 12.3 bar BMEP for MeOH-50. The diesel substitution limits at 3.5 bar BMEP are all misfire (indicated by "MF" on top of the bars), while at the other two loads misfire and knock (indicated by "K") occur. However, knock is the dominant substitution limit for high loads and for the MeOH-W blends of 90% and 100%. The 64% MeOH-W case has misfire as a limit at 10.6 bar BMEP and knock at 12.3 bar BMEP, while for MeOH-50 misfire is the limit at all loads.

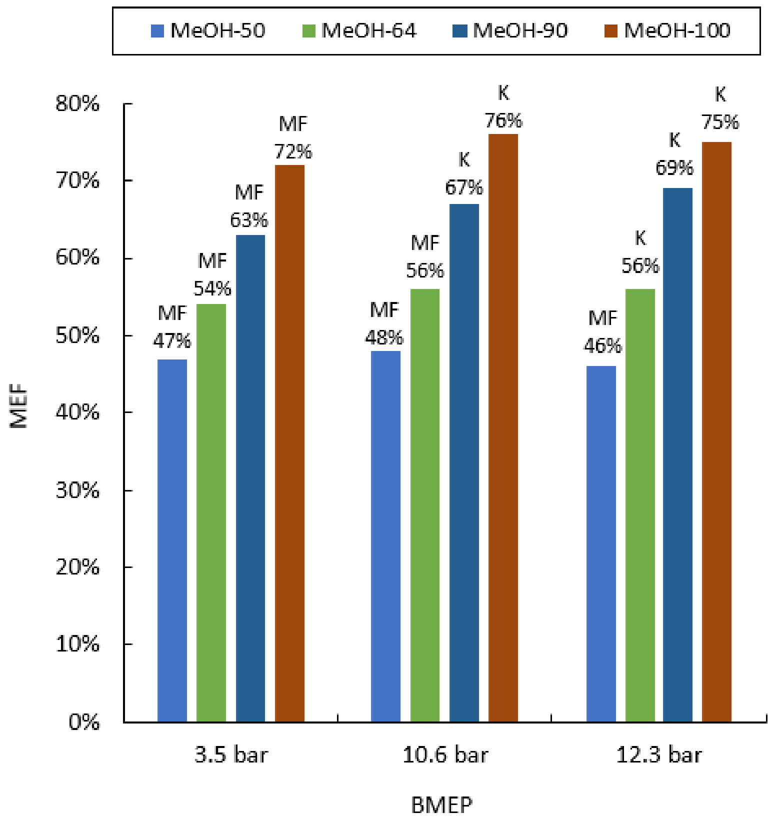

Figure 4: Maximum methanol energy fractions for different load points.

"MF" denotes misfire, and "K" knock.

It can thus be seen that with increasing water content a knock boundary can change into a misfire boundary. This is due to the additional cooling effect of the water, causing the ignition delay to increase and finally to result in a misfire. This phenomenon can be clearly seen on Figure 5 that shows the pressure diagrams at 12.3 bar BMEP for different MeOH-W blends. For MeOH-50 the substitution limit is misfire: a constantly increasing ignition delay can be seen, until diesel stops autoigniting. With higher methanol shares (64%, 90% and 100%) the substitution boundary is knock. From Figure 5 it cannot be distinguished whether it is diesel or methanol knock, but one thing is sure: when the amount of MeOH-W increases, the ignition delay increases. This means that the amount of diesel increases that premixes before autoignition, and thus the total fuel that burns premixed, leading to higher pressures, pressure rise rates and temperatures and thus increasing the possibility for both diesel and methanol knock.

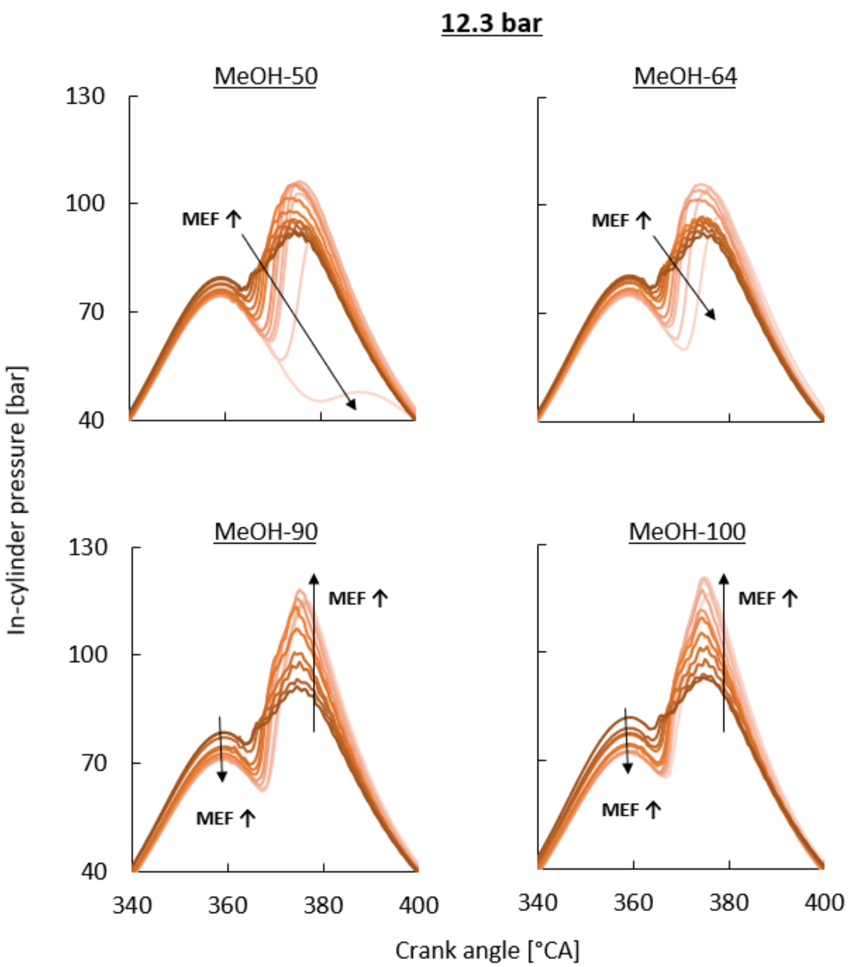

Figure 5: In-cylinder pressures at 12.3 bar BMEP for different MeOH-W blends and MEF.

The lower maximum MEF with increasing water content can be explained by Figure 6, plotting the CA10, a measure for the ignition delay. It can be seen that the CA10 at 12.3 bar BMEP is delaying with higher water content. A delayed CA10 enables at equal MEF that the amount of diesel that premixes during the ignition delay increases. As such, more fuel is burned premixed, resulting in high pressure rise rates and in this way advancing the moment that knock occurs.

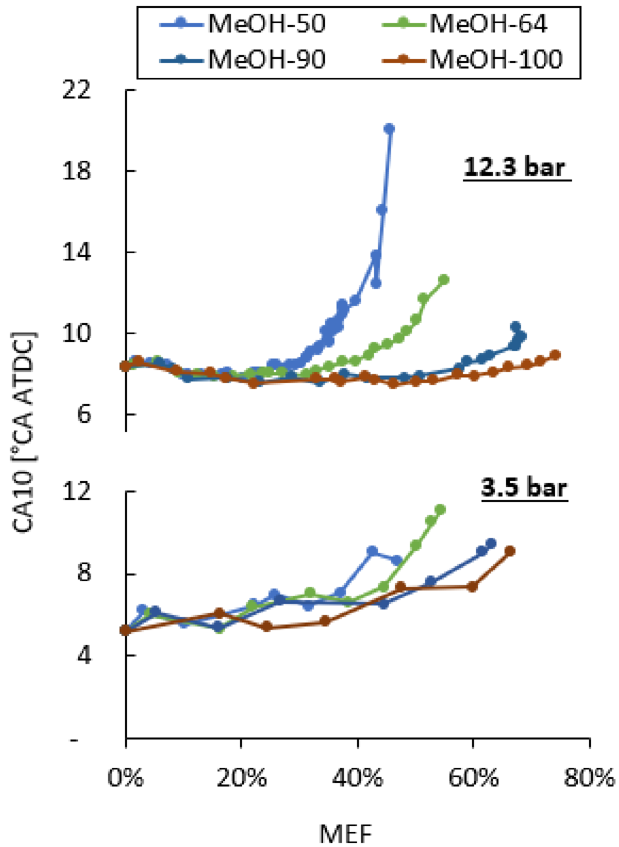

Figure 6: CA10 at 3.5 bar and 12.3 bar BMEP and for different MeOH-W blends and MEF.

One of the objectives of this research was to investigate whether water acts as a knock suppressant. It must thus be observed that the engine tests do not confirm this hypothesis: water does not act as a (diesel or methanol) knock suppressant and as such does not increase the maximum MEF at high loads. Water addition decreases the in-cylinder temperature before combustion as would be expected, but this results in a significant increase in ignition delay during which more diesel mixes with air and MeOH-W. As such, the amount of fuel that burns premixed increases. This leads to high pressure rise rates and high in-cylinder pressures and temperatures. As a consequence the increased ignition delay leads to knock at lower MEF than with pure methanol. However, if the ignition delay gets too high misfire takes place.

If a system could be used with variable start of diesel injection timing (SOI_d), then these effects could be altered. To prevent misfire the following could occur: or (1) the SOI_d could be advanced to make sure the injected diesel ignites and as such misfire is prevented, or (2) the in-cylinder temperatures at TDC and after TDC are too low to enable an autoignition and as such advancing SOI_d has no effect. In case (1) it is also possible that instead of misfire, a knocking event becomes the new diesel substitution limit.

The maximum MEF's in Figure 4 do not indicate the amount of diesel that is substituted, which is an important measure because if green methanol is used, the DSR describes the possible CO_2 savings. On Figure 7 the DSR is plotted against the MEF, as well as a line where DSR = MEF. Assuming that the total injected energy (denominator of the MEF equation, see Section 4.1) remains equal when going from DO to DF operation, a DSR > MEF indicates an increase in efficiency, and a DSR < MEF indicates a decrease. The upper graph is at 3.5 bar BMEP and the lower graph at 12.3 bar BMEP. It can be seen that at both loads, but more pronounced at 3.5 bar BMEP, a higher DSR is reached with more water content. This effect however decreases with increasing MEF.

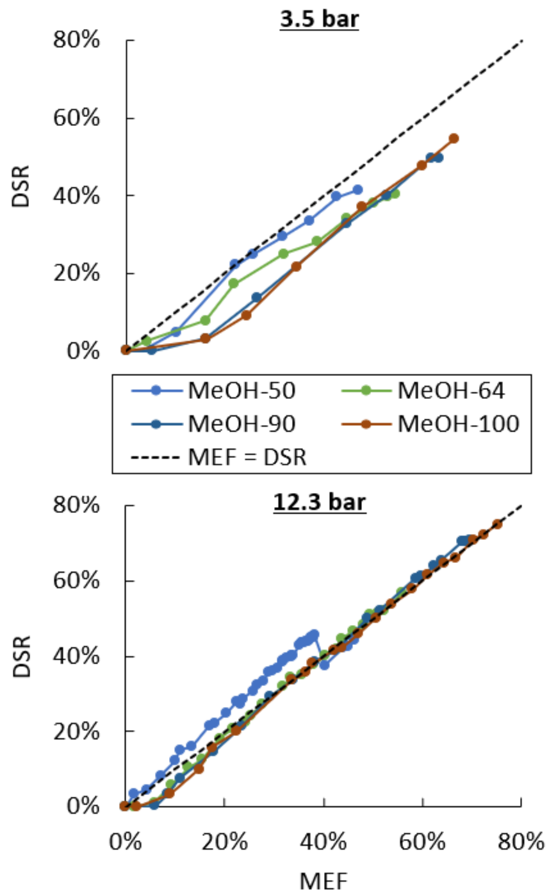

Figure 7: DSR as a function of MEF and for different MeOH-W blends, at 3.5 bar and 12.3 bar BMEP.

5.3 Combustion analysis

In the previous Section, it was pointed out that a higher amount of fuel burns premixed with increasing MeOH and water content. Figure 8 shows the heat release rates (HRR) at 12.3 bar BMEP for different MeOH-W blends and increasing MEF. From the diagrams the increased ignition delay with increasing MEF and water content is clearly visible. For all MeOH-W blends it can be seen that the shape of the heat release rate changes from a bimodal shape to a more unimodal shape. In diesel-only, part of the diesel burns premixed and the majority during the diffusive combustion phase, with a clear distinction between both phases and hence a bimodal shape. In dual-fuel, the combustion is more complex and combines characteristics from both CI and SI operation. In DF mode, diesel autoignition initiates the combustion and the diesel that was mixed with air and methanol during the ignition delay burns premixed. The diesel ignition at multiple locations (as diesel has multiple jets from multiple nozzles) initiates the ignition of the methanol-air mixture and starts the flame propagation throughout this mixture. This means that three combustion types occur: (1) combustion of the premixed diesel-air with entrained methanol, (2) combustion by flame propagation of the methanol-air mixture, (3) diffusive combustion of the injected diesel after (1) took place. From Figure 8 it can be deduced that the more unimodal the HRR shape is, the more fuel is burned simultaneously with a lower distinction between the different phases as in diesel-only operation.

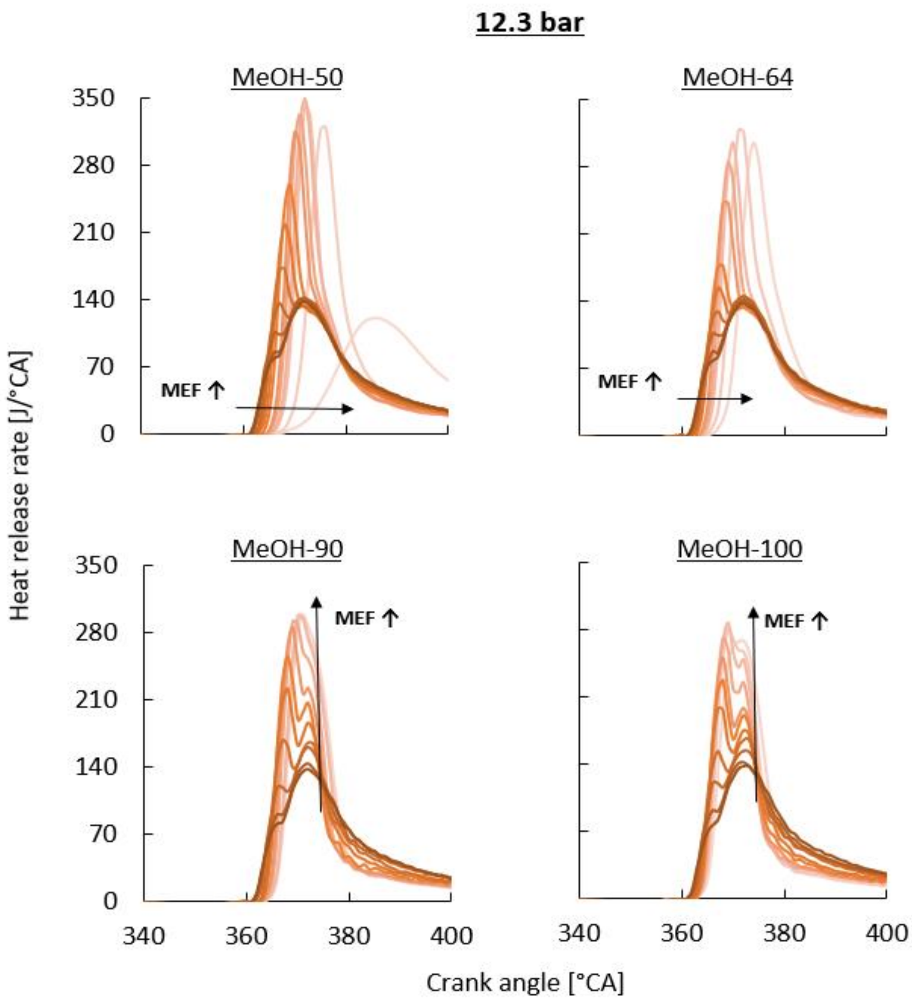

Figure 8: Heat release rate at 12.3 bar BMEP for different MeOH-W blends and MEF.

The observation that more fuel burns simultaneously with as a consequence a more rapid combustion is strengthened by Figure 9 that shows the combustion duration at 3.5 bar and 10.6 bar BMEP. It can be seen that both at low and high load the combustion duration decreases strongly with increasing MEF. At 3.5 bar BMEP and for MeOH-50/64/90, the combustion duration is slightly shorter at low MEFs with more water content and about equal for high MEF. It is assumed that a trade-off takes place. The more water, the longer the ignition delay and the more diesel that burns in the above defined combustion type (1). For higher MEF, this effect is lower as less diesel is injected, and combustion type (2) becomes more dominant. As water is seen as an inert medium not taking part in the combustion, it slows down the methanol flame propagation at high MEF [4].

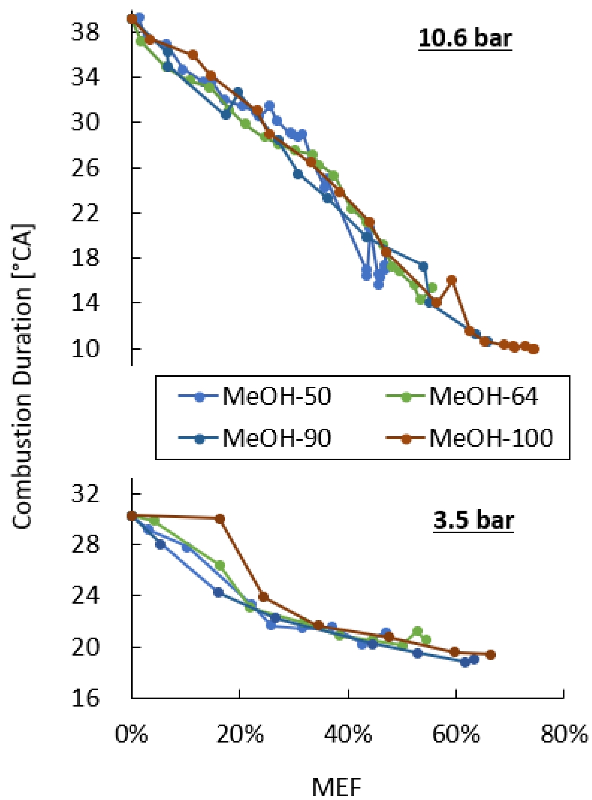

Figure 9: Combustion duration at 3.5 bar and 10.6 bar BMEP for different MeOH-W blends and MEF.

5.4 Brake thermal efficiency

The brake thermal efficiency (BTE) is defined as the useful power compared to the total fuel energy in the cylinder, see Section 4.1. Figure 10 shows the BTE for different MeOH-W blends and with increasing MEF at 3.5, 10.6, and 12.3 bar BMEP. The error bars are not shown on the graph to not overload them: they amount to ~0.4%, ~0.2%, and ~0.18% at respectively 3.5, 10.6, and 12.3 bar BMEP. The results are in line with earlier DF research: with increasing MEF the BTE decreases at low load, and increases at high load. With higher water content, however, there is a clear increase in BTE compared to pure methanol. The maximum BTE amounts to up to 45.9% at 12.3 bar BMEP with MeOH-50. This is 3.3% higher than the maximum BTE with pure methanol and 4.9% higher than in DO. On average, the BTE with MeOH-50 at 12.3 bar BMEP is 2% higher than with MeOH-100. At 10.6 bar BMEP this is 3%, and at 3.5 bar BMEP 4%.

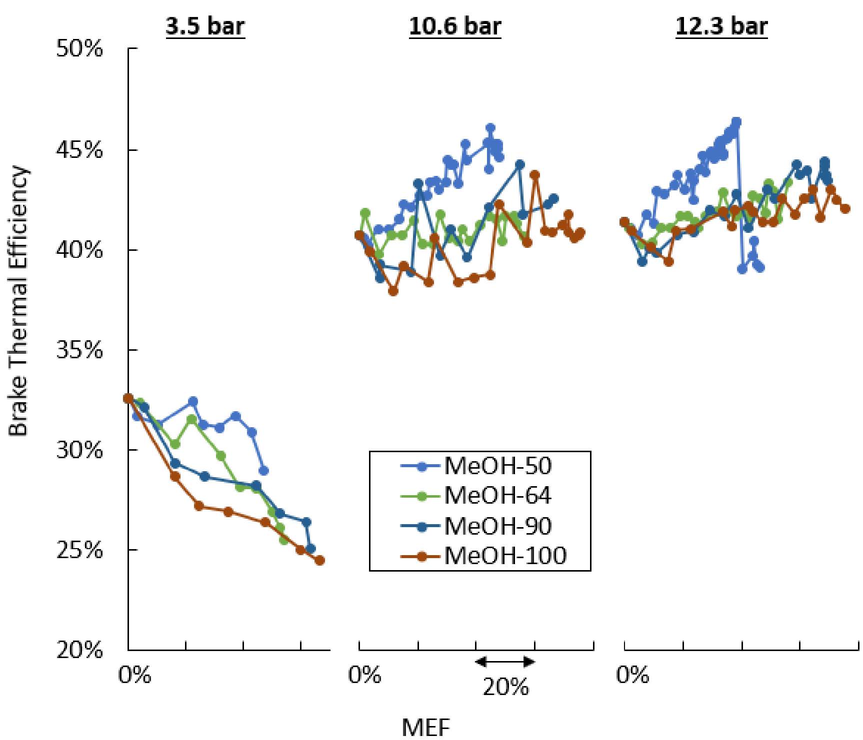

Figure 10: Brake thermal efficiency at 3.5, 10.6 and 12.3 bar BMEP for different MeOH-W blends and MEF.

An explanation for this behavior with increasing water content can be found by plotting the CA50, see Figure 11. It can be seen that the CA50 for different MEF at 10.6 bar BMEP (at 12.3 bar BMEP this is similar) advances to earlier °CA after top dead center (ATDC). This advance happens until a certain MEF, beyond which - depending on the water content - the CA50 starts to retard again due to the increased ignition delay. This fact, together with a later CA10 (see Figure 6) and with a shorter combustion duration (see Figure 9), means that there is a more isochoric combustion closer to TDC, thus leading to higher BTE. The reason thus that the BTE is higher with MeOH-50 is the more optimally phased combustion than with pure methanol.

It can be seen as well that the CA50 in DO is about 17°CA ATDC. Typically, in DO an optimal efficiency is reached with a CA50 around 8 to 10°CA ATDC, so it can be deduced that the current timing was delayed to limit NO_x emissions. Indeed, as will be seen in Section 4.5, NO_x are below the Tier II limit of 8.2 g/kWh (calculated at 1500 rpm) in DO operation.

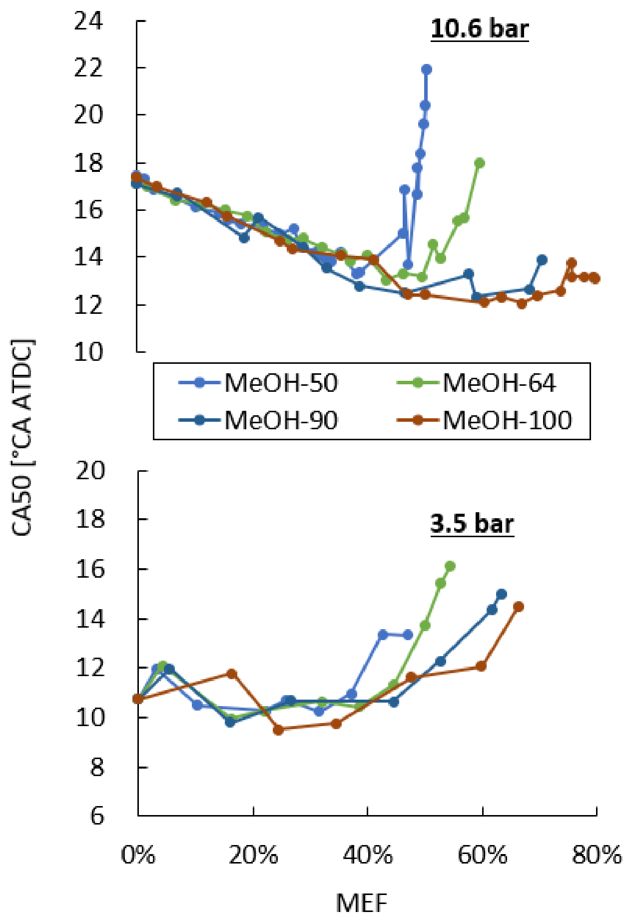

Figure 11: CA50 at 3.5 bar and 10.6 bar BMEP for different MeOH-W blends and MEF.

It can be further seen from Figure 10 that the BTE for MeOH-90 is slightly higher than with pure methanol. On average 1.6%, 0.8% and 0.7% higher for respectively 3.5, 10.6, and 12.3 bar BMEP. Taking into account the error on the BTE of respectively 0.4%, 0.2% and 0.18%, this is only a slightly higher BTE, but still significant.

5.5 NO_x emissions

The NO_x emissions are shown on Figure 12 at 3.5, 10.6, and 12.3 bar BMEP. As can be seen the specific NO_x emissions are highest at 3.5 bar BMEP, but decrease significantly with increasing MEF to well below 2 g/kWh as of an MEF between 10% and 25% depending on the water content. It can be further seen that there is a significant decrease in NO_x emissions with increasing water content. On average the NO_x

emissions are more than 30% lower for MeOH-50 and MeOH-64 than for pure methanol, and about 11% lower for MeOH-90. At low load, water is thus a highly effective measure to decrease NO_x emissions.

At 12.3 bar BMEP, the NO_x emissions decrease with increasing water content. At 10.6 bar BMEP it is remarkable that the NO_x emissions with MeOH-90 are higher than for pure methanol. At 12.3 bar BMEP there is a switching point where the NO_x emissions become higher with MeOH-90 than with pure methanol around a MEF of 40%. For 10.6 and 12.3 bar BMEP the NO_x emissions for MeOH-50 and MeOH-64 are well below the Tier III limit. So it can be stated that water contents of 36% and 50% by weight are at high load an effective measure to meet Tier III emission legislation. At 12.3 bar BMEP, the NO_x emissions are on average 39% and 32% lower for respectively MeOH-50 and MeOH-64 compared to pure methanol, and on average about equal for MeOH-90 compared to pure methanol.

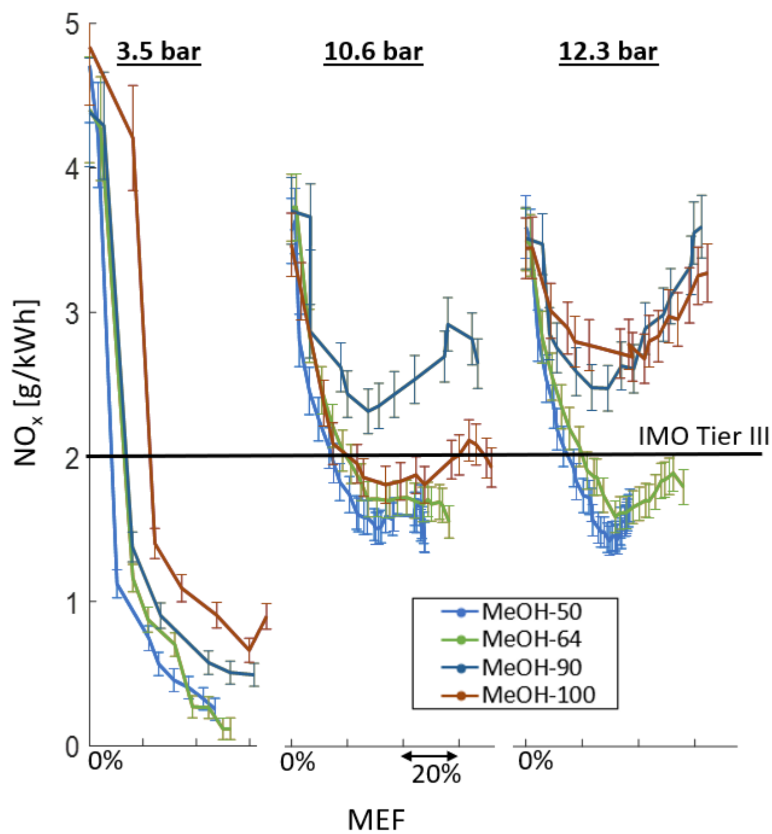

Figure 12: Specific NO_x emissions at 3.5, 10.6 and 12.3 bar BMEP for different MeOH-W blends and MEF.

It can be noticed as well that the NO_x emissions have a parabolic shape at high load as a function of MEF for each MeOH-W blend. In earlier research on this engine [17] [21], this was explained as follows. A first effect (1) that occurs with increasing MEF is the cooling effect of methanol resulting in lower temperatures at the start of combustion and reducing NO_x. A second effect (2) is the more lean combustion as more fuel burns in the premixed combustion phase decreasing NO_x. As of a certain MEF however, a third effect (3) comes into play, namely high peak temperatures as a result of the very rapid combustion due to the increased ignition delay effect (see previous Sections). This third effect becomes dominant as of a certain moment over effects (1) and (2), in this way increasing again the NO_x emissions. This can be seen on Figure 13 that shows the peak in-cylinder temperatures. As can be seen this temperature rises at 10.6 and 12.3 bar BMEP significantly with increasing MEF. For MeOH-W blends with higher water content, the peak temperatures are slightly lower than for low water content MeOH-W blends, but still an increase as a function of MEF is noticed. The high peak temperatures are responsible for effect (3) to become dominant over effect (1) and (2) as of a certain MEF.

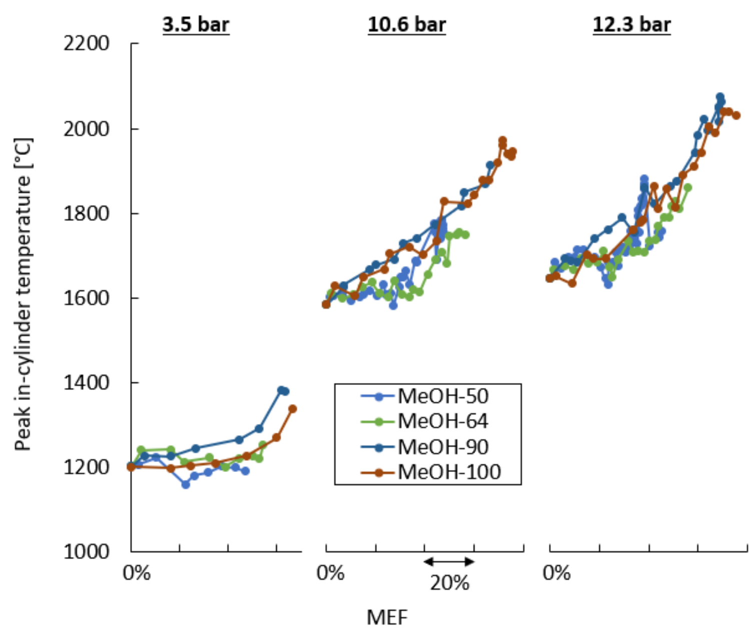

Figure 13:Peak in-cylinder temperature at 3.5, 10.6 and 12.3 bar BMEP for different MeOH-W blends and MEF.

6. Conclusions

It was found that water did not act as a knock suppressant. With increasing water content the maximum MEF went down significantly, e.g. from 75% (with MeOH-100) to 46% (with MeOH-50) at 12.3 bar BMEP. This was due to the fact that with increasing water content the ignition delay increased significantly, resulting in a very rapid combustion of premixed diesel and MeOH-W with high peak pressure rise rates (PPRR) and in-cylinder temperatures. With higher PPRR diesel and methanol knock took place earlier, resulting in lower maximum diesel substitution limits.

NO_x emissions were additionally reduced with increasing water content. At 3.5 bar BMEP, IMO Tier III was reached for MEFs higher than 10-25% (depending on the MeOH-W blend). At 10.6 and 12.3 bar BMEP Tier III was met for MeOH-50 and MeOH-64 as of MEFs of 20%, while for MeOH-90 only between MEFs of 20% and 60%. At high load, adding sufficient water to methanol is thus important to meet IMO Tier III.

The brake thermal efficiency (BTE) with MeOH-90 was slightly but significantly higher than with pure methanol. This is thanks to the additional cooling of water making the combustion more isochoric (more rapid combustion); and also down to the constant start of diesel injection (which was not optimized for the base engine towards efficiency but rather to reach NO_x Tier II limitations) enabling improvements in the combustion phasing. It was even seen that the BTE further increased for blends with higher water content. The maximum BTE was reached with MeOH-50 (while meeting IMO Tier III) at 12.3 bar BMEP at a MEF of 38% amounting to 45.9%, which is 3.3% higher than the maximum BTE with pure methanol, and 4.9% higher than in diesel only operation.

Wrapping up, it can be concluded that methanol-water blends have interesting benefits, on the one hand to reach high BTE while simultaneously reducing fuel production costs, and on the other hand to obtain low NO_x emissions to meet emission legislation.

Acknowledgments

The research in this paper has received funding from the Flanders organization for Innovation and Entrepreneurship (VLAIO) and Anglo Belgian Corporation nv. (Baekeland HBC.2019.2574), and from the European's Horizon 2020 research and innovation programme by means of the projects FASTWATER (Contract No. 860251) and LeanShips (Contract No. 636146). Volvo Penta Benelux is acknowledged for providing the base test engine and for their support. A special acknowledgment for Koen Chielens, the engine technician of the research group Transport Technology at Ghent University, for realizing the mechanical conversions on the Volvo Penta engine.

References

[1] S. Sirimanne, J. Hoffmann and e. al., Review of Maritime Transport 2021, United Nations Conference for Trade and Development, UNCTAD, 2021.

[2] J. Faber, S. Hanayama, S. Zhang and e. al., Fourth IMO GHG Study 2020, London: International Maritime Organization, 2021.

[3] L. Hammer, M. Eide, M. Leisner and e. al., DNV Maritime Forecast to 2050 - Energy Transition Outlook 2021, DNV GL, 2021.

[4] S. Verhelst, J. Turner, L. Sileghem and J. Vancoillie, "Methanol as a Fuel for Internal Combustion Engines," *Elsevier - Progress in Energy and Combustion Science,* vol. 70, pp. 43-88, 2019.

[5] Z. Tian, Y. Wang, X. Zhen and Z. Liu, "The effect of methanol production and application in internal combustion engines on emissions in the context of carbon neutrality: A review.," *Elsevier - FUEL,* vol. 320, no. 123902, 2022.

[6] G. Olah, "After Oil and Gas: Methanol Economy," Catalys Letters, 93, 2004.

[7] R. Pearson and J. Turner, "Renewable Fuels - An Automotive Perspective," *Elsevier - Comprehensive Renewable Energy*, pp. 305-342, 2012.

[8] F. Lonis, V. Tola and G. Cau, "Assessment of integrated energy systems for the production and use of renewable methanol by water electrolysis and CO2 hydrogenation," *Elsevier - FUEL*, vol. 285, no. 119160, 2021.

[9] P. Gautam, Neha, S. Upadhyay and S. Dubey, "Bio-methanol as a renewable fuel from waste biomass: Current trends and future perspective," *Elsevier - FUEL*, vol. 273, no. 117783, 2020.

[10] A. Basile and F. Dalena, Methanol: Science and Engineering, Elsevier, 2018.

[11] A. Agarwal, H. Valera, M. Pexa and J. Cedik, Methanol: A Sustainable Transport Fuel for CI Engines, Springer, 2021.

[12] C. Yao, W. Pan and A. Yao, "Methanol fumigation in compression-ignition engines: a critical review of recent academic and technological developments," *Elsevier - FUEL*, vol. 209, pp. 713-732, 2017.

[13] J. Coulier and S. Verhelst, "Using Alcohol Fuels in Dual Fuel Operation of Compression Ignition Engines: A Review," in *CIMAC Congress*, Helsinki, 2016.

[14] J. Dierickx, S. Verhelst and et al., "Strategies for introducing methanol as an alternative fuel for shipping," in *Transport Research Arena Conference, TRA*, Vienna, 2018.

[15] S. Mayer, J. Sjöholm and T. Murakami, "Performance and emission results from the MAN B&W LGI Low-Speed Engine Operating on Methanol," in *CIMAC Congress*, Helsinki, 2016.

[16] T. Stojcevski, D. Jay and L. Vicenzi, "Operation Experience of World's First Methanol Engine in a Ferry Installation," in *CIMAC Congress*, Helsinki, 2016.

[17] J. Dierickx, L. Sileghem and S. Verhelst, "Efficiency and Emissions of a High-Speed Marine Diesel Engine Converted to Dual-Fuel Operation with Methanol," in *CIMAC Congress*, Vancouver, 2019.

[18] Y.-H. Pu, K. Christianen, P. Molander and S. Verhelst, "The FASTWATER Demonstrator: Retrofitting a Harbor Tug Boat to Methanol/MGO Dual-Fuel Operation," in *Transport Research Arena Conference, TRA*, Lisbon, 2022.

[19] FASTWATER, "FAST Track to Clean and Carbon-Neutral WATERborne Transport," 2020. [Online]. Available: https://www.fastwater.eu/.

[20] L. Mattheeuws, "ABC's Dual-Fuel Engines Running on Renewable Fuels like Methanol and Hydrogen," in *CIMAC Congress*, Vancouver, 2019.

[21] J. Dierickx, L. Sileghem and S. Verhelst, "Retrofitting a high-speed marine engine to dual-fuel methanol-diesel operation: A comparison of multiple and single point methanol port injection," *Elsevier - FUEL Communications,* 2021.

[22] Q. Wang, L. Wei, W. Pan and C. Yao, "Investigation of Operating Range in a Methanol Fumigated Diesel Engine," *Elsevier - FUEL,* vol. 140, pp. 164-170, 2015.

[23] B. Wang, C. Yao, C. Chen, J. Feng, H. Lu and L. Feng, "To extend the operating range of high MSP with ultra-low emissions for DMDF unit pump engine," *Elsevier - FUEL,* vol. 218, pp. 295-305, 2018.

[24] Z. Chen, J. He, H. Chen, L. Wang and L. Geng, "Experimental study of the effects of spark timing and water injection on combustion and emissions of a heavy-duty natural gas engine,," *Elsevier - FUEL,* vol. 276, no. 118025, 2020.

[25] A. Li, Z. Zheng and T. Peng, "Effect of water injection on the knock, combustion, and emissions of a direct injection gasoline engine," *Elsevier - FUEL,* vol. 268, no. 117376, 2020.

[26] P. Ni, X. Wang and H. Li, "A review on regulations, current status, effects and reduction strategies of emissions for marine diesel engines," *Elsevier - FUEL,* vol. 279, no. 118477, 2020.

[27] S. Zhu, B. Hu, J. Bernards, C. Branney and e. al., "A review of water injection applied on the internal combustion engine," *Elsevier - Energy Conversion and Management,* vol. 184, pp. 139-158, 2019.

[28] X. Sun, J. Ning, X. Liang, G. Jing, Y. Chen and G. Chen, "Effect of direct water injection on combustion and emissions characteristics of marine diesel engines," *Elsevier - FUEL,* vol. 309, no. 122213, 2022.

[29] L. Sileghem, J. Vancoillie and S. Verhelst, "Performance and Emissions of a SI Engine using Methanol-Water Blends," *SAE International,* 2013.

[30] S. Mayer, "NOx Reduction to Tier III Levels on MAN B&W LGI Low-Speed Engines by Water Addition to Either Methanol or Conventional Diesel Fuel Oil," in *CIMAC Congress*, Vancouver, 2019.

[31] C. Xu and H. Cho, "Effect of Methanol/Water mixed Fuel Compound Injection on Engine Combustion and Emissions," *MDPI - Energies,* vol. 14, no. 4491, 2021.

[32] M. Svanberg, J. Ellis, J. Lundgren and I. Landälv, "Renewable methanol as a fuel for the shipping industry," *Elsevier - Renewable and Sustainable Energy Reviews,* vol. 94, pp. 1217-1228, 2018.

[33] L. Carvalho, J. Lundgren, E. Wetterlund, J. Wolf and E. Furusjo, "Methanol production via black liqur co-gasification with expanded raw material base - Techno-economic assessment," *Elsevier - Applied Energy,* vol. 225, pp. 570-584, 2018.

[34] T. Johansen and J. Schramm, "Low-temperature miscibility of ethanol-gasoline-water blends in flex fuel applications," *Energy Sources, Part A: Recovery, Utilization, and Environmental Effects,* vol. 31, no. 18, pp. 1634-1645, 2009.

[35] H. Keuken, T. MacDonald and E. de Jager, "Hydrous ethanol for gasoline blending," in *17th International Symposium on Alcohol Fuels*, Tiayuan China, 2008.

[36] IMO, "MARPOL/CONF./3.34 - Protocol of 1997 and Annex VI to MARPOL 73/78 as adopted by the Conference," International Maritime Organization, 1997.

[37] J. Taylor, "An introduction to erro analysis," *Sausalito, CA: University Science Books,* 1997.

[38] F. Lonis, V. Tola and G. Cau, "Assessment of integrated energy systems for the production and use of renewable methanol by water electrolysis and CO2 hydrogenation," *Elsevier - FUEL,* vol. 285, no. 119160, 2021.

[39] V. Dieterich, A. Buttler, A. Hanel, H. Spliethoff and S. Fendt, "Power-to-liquid via synthesis of methanol, DME or Fischer-Tropsch-fuels: a review," *Energy Environmental Science,* vol. 13, no. 10, pp. 3207-3252, 2020.

[40] J. Ott, V. Gronemann, F. Pontzen, E. Fiedler, G. Grossmann and e. al., "Methanol," *ULLMANN's Encyclopedia of industrial chemistry,* 2012.